Geophysical Prospecting **37**, 647–668, 1989

SPONTANEOUS POTENTIALS AND RESISTIVITY SURVEYS APPLIED TO HYDROGEOLOGY IN A VOLCANIC AREA: CASE HISTORY OF THE CHAÎNE DES PUYS (PUY-DE-DÔME, FRANCE)[1]

CLAUDE FOURNIER[2]

ABSTRACT

FOURNIER, C. 1989. Spontaneous potentials and resitivity surveys applied to hydrogeology in a volcanic area: case history of the Chaîne des Puys (Puy-de-Dôme, France). *Geophysical Prospecting* **37**, 647–668.

Two geophysical methods [resistivity soundings and spontaneous potentials (SP)] are used to investigate aquifers in the Quaternary volcanic formations of the Chaîne des Puys (France). The interpretation of the resistivity soundings required a specific work of determination of the resistivity of the formations concerned. The basement topography, characterized by axial horst and graben structures and perpendicular palaeovalleys, was revealed. SP was developed experimentally in the field and theoretically. It is shown that the SP anomalies can be considered as double-layer potentials, with their source on the aquifers' interfaces. The most significant of them is the water table, which creates an SP anomaly of similar but inverted form. SP anomalies due to flows in unconfined aquifers, in palaeovalleys, and in volcanic ranges are computed and compared with the observed ones. These two methods have determined the extent and the boundary conditions of the different hydrogeological basins and have determined the major drainage axes and the groundwater flow pattern.

INTRODUCTION

In the northern part of the Chaîne des Puys (Puy-de-Dôme, France) (Fig. 1), volcanic aquifers supply about 80000 people with drinkable water. After the severe drought of the summer of 1976, the Ministry of Agriculture wanted to know more

[1] Received July 1987, revision accepted October 1988.

[2] Present address: United Nations Development Program, P.O. Box 553, Banjul, The Gambia. Formerly: Observatoire de Physique du Globe de Clermont-Ferrand, and Centre Géologique et Géophysique, Université de Sciences et Techniques du Languedoc, Montpellier, France.

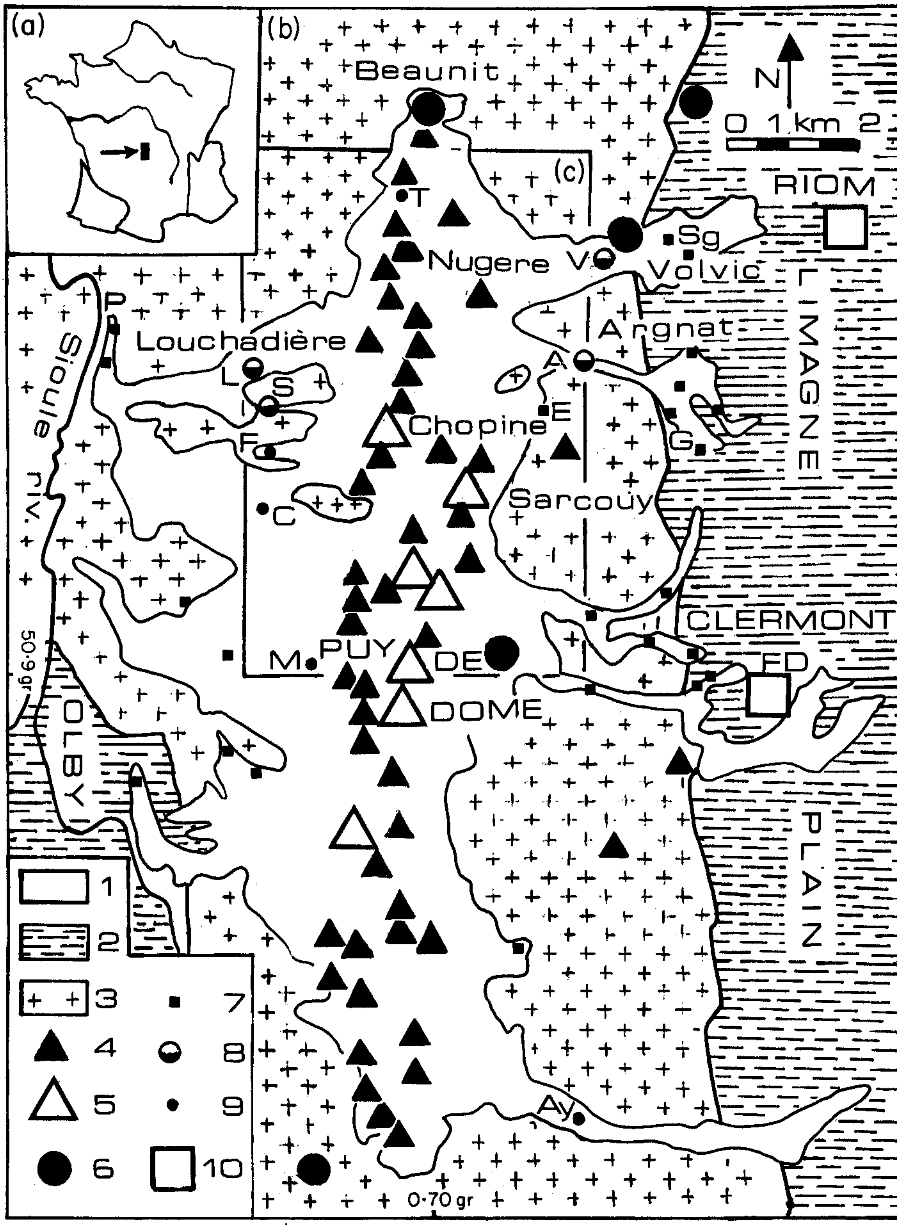

FIG. 1. (a) Location map of the Chaîne des Puys. (b) Simplified geological map of the Chaîne des Puys. The symbols indicate: (1) volcanic cover, (2) detrital rocks filling up the grabens, (3) crystalline and metamorphic basement, (4) Strombolian cones, (5) trachytic domes or peaks, (6) basaltic maar, (7) springs [A: Argnat; E: Egaules; P: Peschadoire; Sg: St Genest l'Enfant], (8) catchment galleries [A: Argnat; L: Louchadière; S: Sérange; V: Volvic], (9) boreholes or wells [Ay: Aydat; C: Côme; F: Fontêtes; M: Bac de Montmeyre; T: Thiollet], and (10) major cities. (c) Frame of the map in Fig. 4.

about these precious resources in order to better manage and protect them. The Observatoire de Physique du Globe de Clermont-Ferrand was asked to do a systematic geophysical survey. Two methods were employed: Schlumberger resistivity soundings and spontaneous potential (SP) measurements. Resistivity soundings revealed important structures below the volcanic rocks. The use of the SP method in this context led to important theoretical and methodological developments.

Geological Presentation

The Chaîne des Puys is a north–south chain of about sixty Quaternary volcanoes (with an activity range from 12 000 to 4000 years BC) established on a horst structure of Hercynian basement rocks (Camus 1975) (Fig. 2). On each side of the horst, two asymmetric grabens (Limagne plain and Olby trough) are partially filled with post-Oligocene detrital rocks. These two types of formations are impermeable except for certain superficial levels of limited extension. The acid volcanic products of the trachytic domes (Puy de Dôme, Sarcouy) and peaks (Chopine) are also impermeable. On the other hand, basic and intermediate volcanic materials are granular (pyroclastics and scorias in the Strombolian cones or intercalated within lava flows) or are fractured by cooling processes (columnar lava flows) and are therefore notably permeable. Belkessa (1977) has measured permeabilities from 10^{-3} to 3×10^{-5}m/s in lava flows of the area.

Rain percolates through the cones and lava flows and accumulates on the impermeable basement. The flow of these unconfined aquifers is principally controlled by the basement's topography, ridges which may obstruct it, and palaeovalleys which drain toward the end of the lava flows where they supply numerous springs (St Genest, Peschadoire). In order to harness the waters upstream of the villages supplied Volvic, Argnat and La Louchadière galleries have successfully been sunk

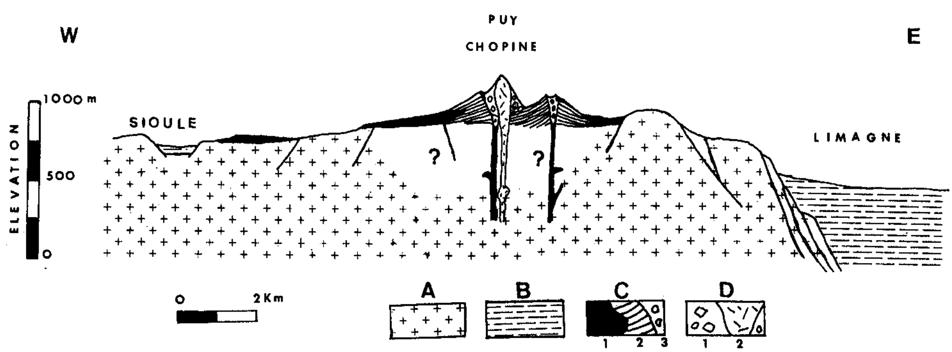

FIG. 2. Transverse cross-section of the Chaîne des Puys at the latitude of Puy Chopine. The symbols indicate: (A) crystalline and metamorphic basement, (B) sedimentary formations, (C) basic volcanic formations [1: basalt lava flows; 2: pyroclastics; 3: pyroclastic breccia], and (D) acid volcanic formations [1: trachytic breccia; 2: trachytic lava plug].

up to the thalweg of their respective palaeovalleys. More recently and further upstream, boreholes have been drilled in addition (Cheyre de Côme, Thiollet). Sometimes boreholes have also caught water trapped in basaltic maar structures (Beaunit) (Aubert, Camus and Fournier 1984).

Resistivity Surveys

Schlumberger resistivity soundings benefit from favourable conditions on the Chaîne des Puys: volcanic formations of high resistivity cover a largely more conductive basement. Specific determinations of the true resistivity of the different formations were obtained by completing resistivity soundings close to boreholes with a recorded lithology (Fig. 3a) or above qualitatively well-known structure, e.g. palaeovalleys (Fig. 3b) or large Strombolian cones of saturated pyroclastics covered by a desaturated and decompressed one (Fig. 3c). The resistivities obtained from the 57 resistivity soundings carried out are summarized in Table 1. Plotting an isohypse map of the top of the basement revealed the existence of an axial graben in the northern part of the Chaîne des Puys and a horst in the central part (Figs. 4 and 12a). The delimitations of these structures by Aubert and Camus (1974) have been partially modified. Some faults with orientation N10° to N40° and their conjugated fractures have controlled the formation of these structures and have later facilitated the rise of magma, as is shown by the alignment of volcanoes linked to some of them. Between these two events a probably plio-quaternary hydrological system partially eroded both the horst and graben structures. Along the channels of their respective palaeovalleys, the galleries of Argnat and Volvic drain the water stored in the axial graben, which appears to be the principal underground reservoir. The other catchments are supplied by independent hydrogeological basins separated from each other by basement ridges. However, the limits and the independence of certain systems (Egaules, Fontêtes) are still difficult to determine accurately.

Table 1. Resistivity (in Ωm) of the formations of the Chaîne des Puys.

Lava flows (Hawaiites)	Dry: 10 560 (8820–12 640) Water-saturated: 1480 (1300–1680) Altered: 570 (470–680)
Pyroclastics	Dry: 32 110 (29 600–34 850) Water-saturated: 10 310 (8060–13 190)
Trachytic breccia	1300 (360–1700)
Basement	Unaltered: 2160 (1610–2890) Altered: 620 (460–840)

The data follow a log-normal distribution. The first figure is the average resistivity; the limits of the 68% confidence interval are indicated.

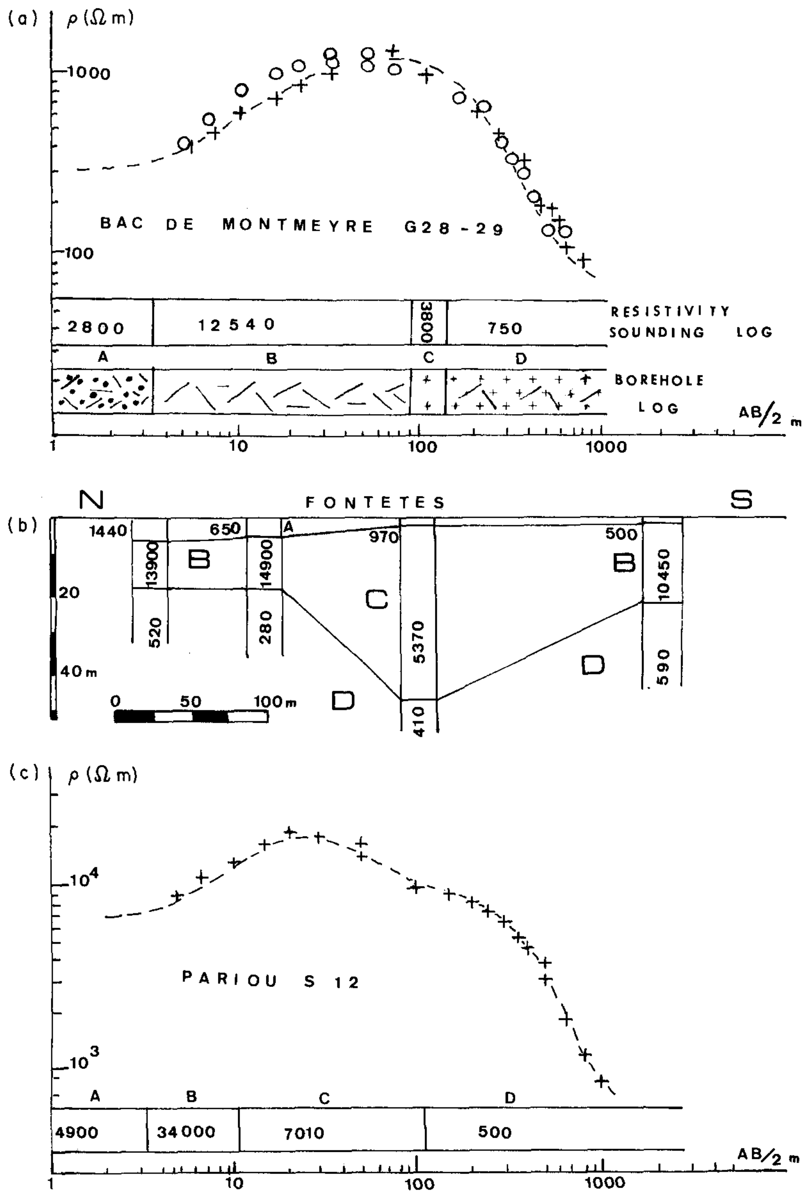

FIG. 3. Bac de Montmeyre. (a) Borehole log: A: scorias, B: dry basalt, C: unfractured syenite, D: fractured syenite. Resistivity sounding field curves and interpretation log for G28 (○○○) orientation east–west, and G29 (+ + +) orientated north–south. (b) Geoletric cross-section across the Fontêtes palaeovalley from resistivity sounding logs (vertical columns). A is topsoil and alterated basalt, B is dry basalt, C is superposition of wet and dry basalt, and D is crystalline basement. (c) Resistivity sounding above a large Strombolian structure (Puy de Pariou) and its interpretation log (horizontal column). A is altered superficial layer, B is dry and compressed pyroclastics, C is wet pyroclastics, and D is crystalline basement. (+ + +) experimental point, (- - -) computed curve.

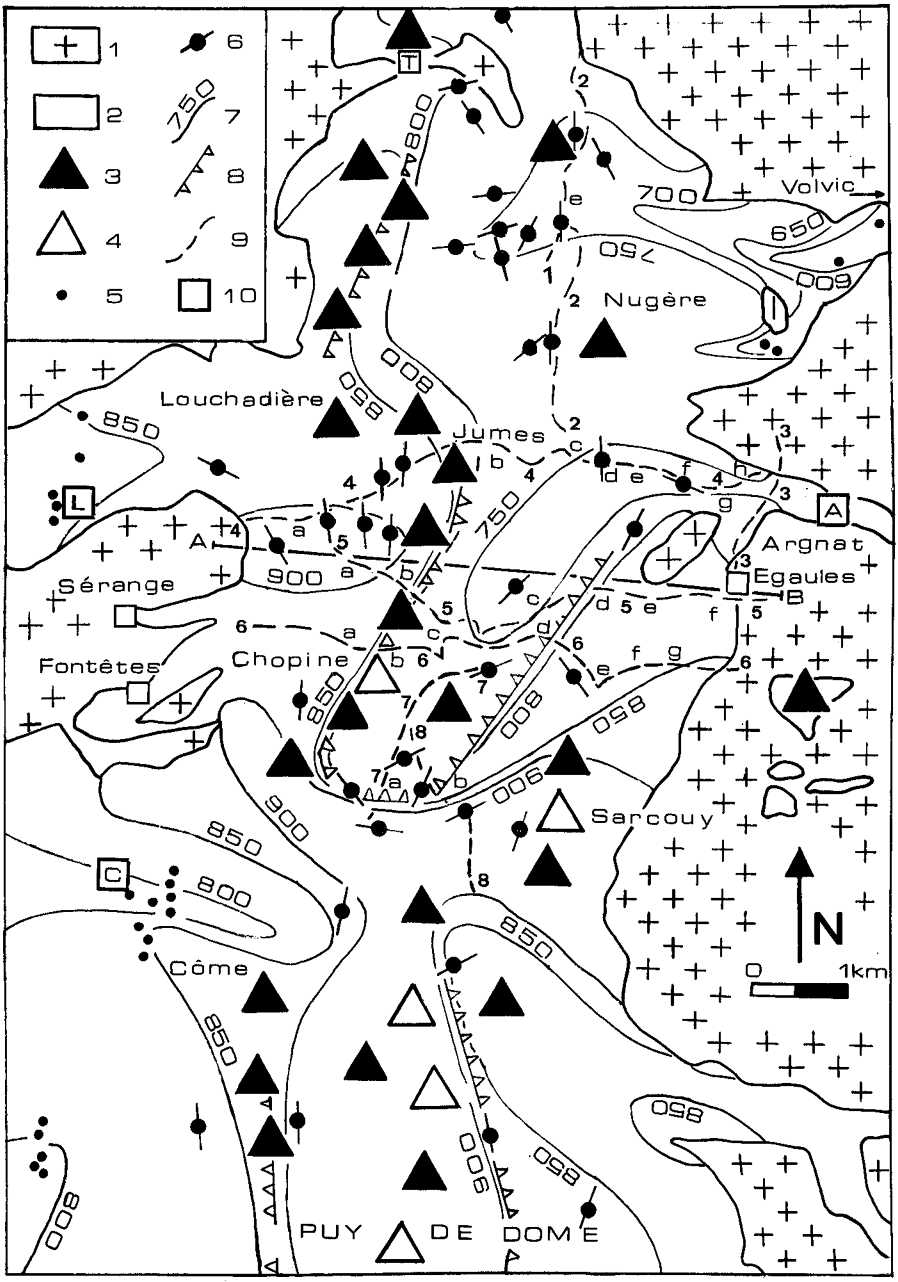

FIG. 4. Hypsometry of the basement according to resistivity soundings. The symbols indicate: (1) crystalline and metamorphic basement, (2) volcanic cover, (3) Strombolian cones, (4) trachytic domes or peaks, (5) boreholes, (6) resistivity soundings, (7) level curves of the top of the basement, with elevation in metres above sea level, (8) probable faults, (9) SP profile (the numbers and letters correspond to the test and the relevant figures thereafter), and (10) groundwater catchment system [A: Argnat gallery; C: Cheyre de Côme borehole; L: Louchadière gallery; T: Thiollet well].

The Spontaneous Potentials Method

The spontaneous potentials method (SP) involves measuring the steady state and natural potentials existing on the ground surface. Among the causes generating such potentials, electrofiltration is the principal phenomenon to be considered in the Chaîne des Puys. An electromotive force (emf) is generated as the flow of water trails the positive ions downstream (Fitterman 1978). Thus the magnitude and the distribution of the potentials at ground level can provide useful information of the underground flow generating them.

Measurements methodology

Copper–copper sulphide electrodes have been used in association with a digital high-input impedance voltmeter ($22 \times 10^6\ \Omega$). Placing the electrodes in 20 cm deep holes reduces the SP effect from chemical and moisture variations in the topsoil. One electrode is left as a reference at a fixed point. The second one is moved (the measuring interval is generally 50 m) as long as the SP remains stable (generally beyond 500 m). Then a new reference point is chosen, with the mean of at least nine independent measurements between the old and the new reference fixing its potential with respect to the old one. The points of reference are arranged to form a network composed of loops. One of these points (A on Fig. 5) is located on granitic basement (i.e. not above groundwater flow) and closed to the studied area (to limit regional effects). It has been attributed a potential equal to zero. Thus all the reference points and all the points linked to each of them have been attributed an SP value with respect to A.

The closing gap of the SP around the loops, the repetition of profiles in the space of a few weeks and the computation of the experimental variogram (Guillaume 1977) of 400 measurements let us estimate their standard deviation to be around 20 mV. The 3000 measured points, covering about 52 km^2, have been plotted as a map of isopotential lines (Fig. 5) with an equidistance of 50 mV.

Computation of SP associated with flow

In a steady state regime, Fitterman (1978) indicated that, with most geological material, a total density of current **i** can be defined as the sum of a 'conductive current' following Ohm's law and a 'convective current' following Helmoltz's law:

$$\mathbf{i} = -\sigma(\nabla \mathbf{V} + C\nabla \mathbf{H}). \tag{1}$$

σ represents the electric conductivity, $\nabla \mathbf{V}$ the electric field vector, and $\nabla \mathbf{H}$ the hydraulic gradient. C is the electrofiltration coupling coefficient.

We assume that the ground can be divided into several zones of homogeneous properties with no current source except electrofiltration. Thus, for each zone:

$$\text{div}\ \mathbf{i} = \nabla^2\psi = 0, \tag{2}$$

$$\mathbf{i} = -\sigma\nabla\psi, \tag{3}$$

$$\Psi = V + CH. \tag{4}$$

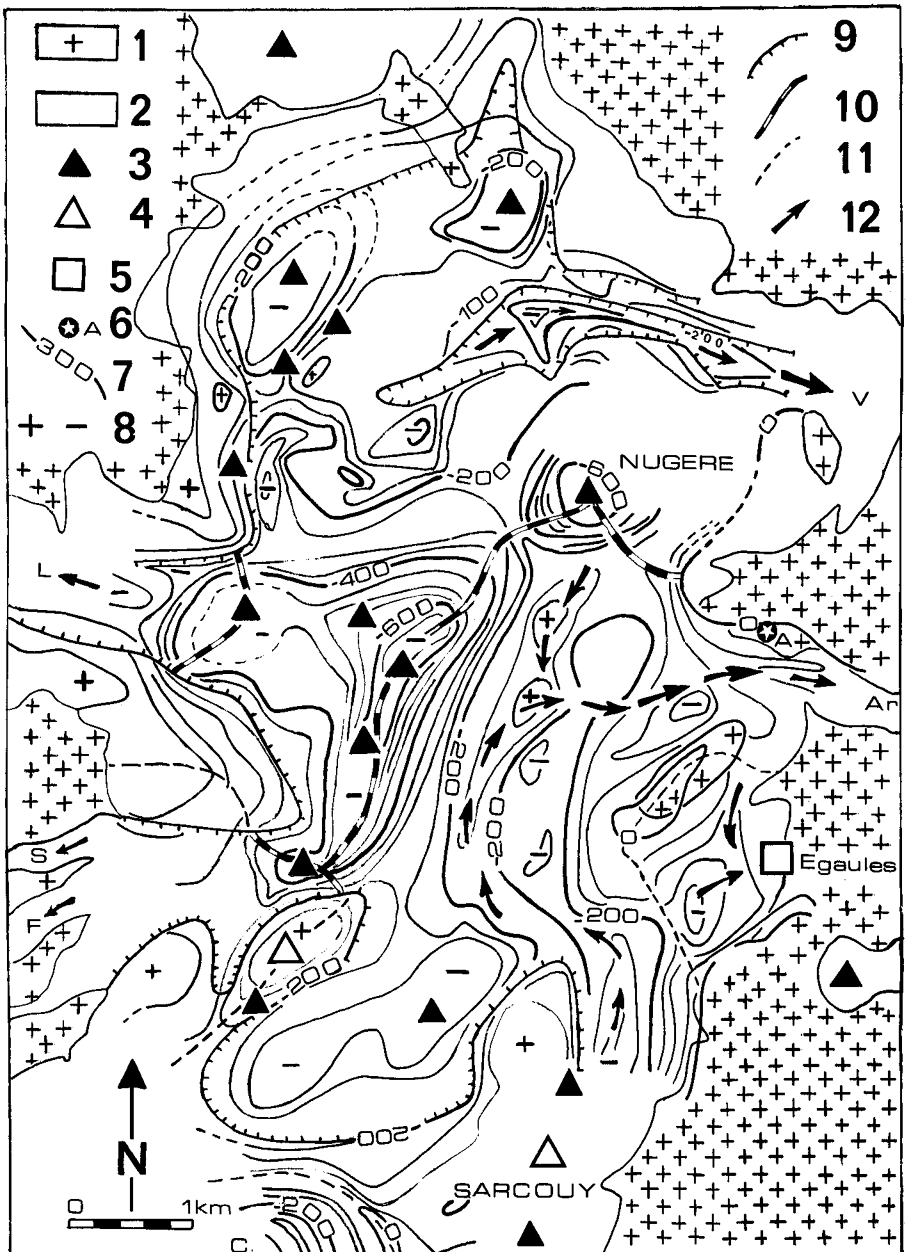

FIG. 5. Spontaneous potentials map of the northern part of the Chaîne des Puys. The symbols indicate: (1) crystalline and metamorphic basement, (2) volcanic cover, (3) Strombolian cones, (4) trachytic domes or peaks, (5) Egaules spring, (6) reference point chosen for SP, (7) line of equal SP, indication of the SP value in mV, (8) relative maximum or minimum SP, (9) lateral limit of the saturated zone, (10) watershed line due to basement's crest, (11) watershed line in the saturated zone, and (12) drainage axis towards the following springs: Ar: Argnat; F: Fontêtes; L: Louchadière; S: Sérange; V: Volvic. For symbols (9)–(12) see also Table 2.

TABLE 2. Hydrogeological interpretation of SP anomalies

Aspect	Location	Hydrogeological significance	Symbol used in Fig. 5
High horizontal SP gradient	On a flat topography	Lateral limit of an unconfined aquifer	9
	On the flank of a volcano	Ascent of the water table in the volcanic cone	None
Minimum of SP	On a flat topography	Palaeovalley axis	12
	On the top or the flank of a volcano	Crest of the water table and underground watershed line	10
Maximum of SP	Above an unconfined aquifer	Depression of the water table due to better drainage	12
	Between two unconfined aquifers	Watershed line due to a crest of the impervious basement	11

Ψ represents the total electric potential, as the sum of the 'conductive' and 'convective' potentials. Through the interface S between two homogeneous zones, 1 and 2, the conductivity and the coupling coefficients can change drastically but V, H, and the component of i perpendicular to S are continuous, so that:

$$\sigma_1 \frac{\partial \Psi_1}{\partial n} = \sigma_2 \frac{\partial \Psi_2}{\partial n}, \tag{5}$$

$$\Psi_2 - \Psi_1 = -(C_2 - C_1)H. \tag{6}$$

Equations (5) and (6) characterize double layer potentials.

If, in addition, we can assume the conductivity to be constant through S, the double layer potential created by S at ground level should be:

$$\Psi = \frac{-(C_2 - C_1)}{2\pi} \iint_S H \frac{\mathbf{r} \cdot \mathbf{n}}{r^3} \mathrm{d}s. \tag{7}$$

For a null hydraulic gradient versus the 0y-axis with the reference system as in Fig. 6a, (7) becomes (8) at ground level:

$$V(x, 0) = -\frac{(C_2 - C_1)}{2\pi} \int_0^L H(x') \frac{[(x - x')\partial h/\partial x' + h(x')]}{(x - x')^2 + h^2(x')} \mathrm{d}x'. \tag{8}$$

We must consider three homogeneous zones – the desaturated zone, the saturated zone, and the aquiclude basement.

The desaturated zone

Electrokinetic phenomena need the saturation of the porous medium. Heavy rain can temporarily saturate thin layers of this zone by descending infiltrated water. Intense thunderstorms (4 mm of rain in 20 min) created SP of less than 5 mV

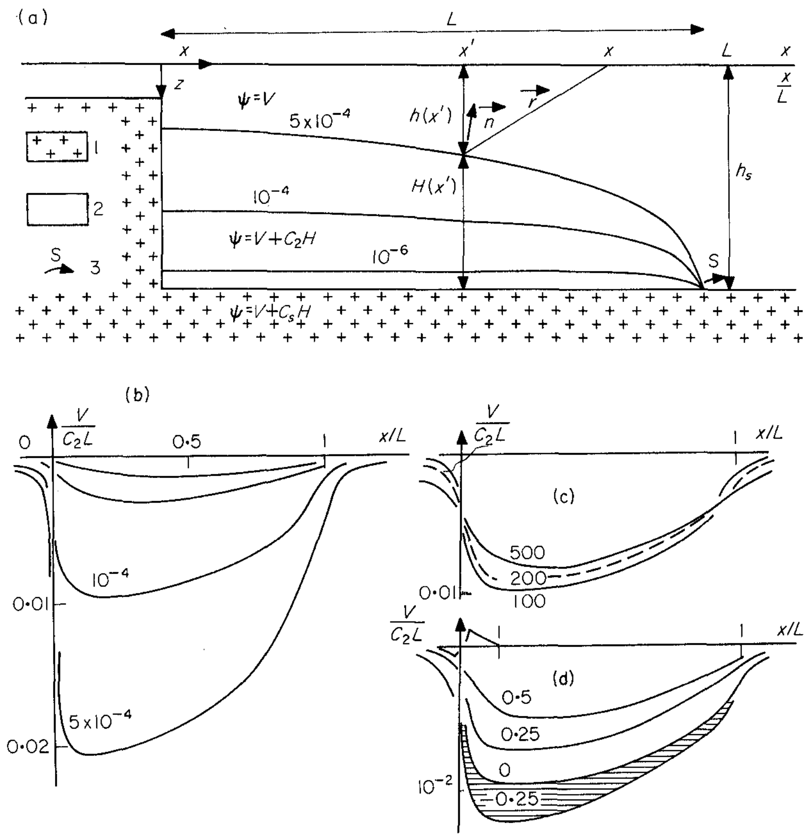

FIG. 6. Unconfined aquifer supplied by its own surface. (a) Proposed model. The symbols indicate: 1: basement; 2: volcanic lava flow; 3: spring. Three water tables are plotted, corresponding to different values of P/K as indicated. The reference system, the parameters, and the expression of Ψ for each zone correspond to (7), (8), (9) and (10) in the text. (b) SP due to different water tables. The corresponding value of P/K is indicated above each curve. (c) SP due to the same water table ($P/K = 10^{-4}$) as a function of the basement's depth (h_s) indicated above each curve. (d) SP due to the water table ($P/K = 10^{-4}$, $h_s = 100$ m) and the aquifer–basement interface for different values of $(C_s - C_2)/C_2$indicated above each curve.

(Fournier 1983). Therefore, the SP produced by this zone can be neglected (i.e. $C_1 = 0$) and V, the potential measured on the ground surface, can be substituted for Ψ in (7) and (8).

The saturated zone

There is no published value of C for volcanic rocks. Ahmad (1961), Ogilvy, Ayed and Bogolovsky (1969) and Coromp *et al.* (1974) worked on different silicious porous materials. For natural waters, they showed that C was almost independent of the permeability but was linearly dependent on the electrical conductivity of the percolating water. For the poorly mineralized waters from the Chaîne des Puys (90–150 μS/cm) we can expect values of C of a few mV/m.

The basement

The basement is within the saturated zone, but its permeability is at least 10 times smaller than the volcanic rock. Barbaud (1983) showed that arenaceous basement waters were 25–50% more resistant than volcanic spring waters. As C does not depend on permeability but on water conductivity, its value can be 1.5 times greater than in the volcanic aquifers. But for granite below a volcanic cover, water mixing between the two formations probably strongly decreases the contrast of C. Consequently, the main and probably the only SP generator appears to be the piezometric surface.

SP due to a free surface aquifer supplied by its own surface

Let us consider an unconfined aquifer within a horizontal lava flow, infinite in the $0y$-direction (Fig. 6a), and drained by a line of springs or a tunnel at a distance L from its upstream limit. Such a limit can be a fault in the basement. Neglecting the vertical component of the flow, the hydraulic head $H(x)$ depends upon the efficient rainfall P and the permeability K (Schoeller 1962):

$$H(x) = \sqrt{\frac{P}{K}(L^2 - x^2)} + h_0, \tag{9}$$

where h_0 is the residual hydraulic head at the spring, depending upon the baseline chosen for the hydraulic head; at present $h_0 = 0$. We can deduce the depth of the water table by

$$h(x) = h_s - H(x) + h_0, \tag{10}$$

where h_s is the depth of the basement. Equations (8)–(10) yield the potential V_1 created by the water table using Simpson's method. Note that the theoretical SP is negative with a zone of high SP gradient, corresponding to the upstream limit of the aquifer (Fig. 6b). The rest of the SP curve reproduces the reverse shape of the water table. Deepening a similar aquifer by increasing h_s smoothes the theoretical anomaly but does not greatly affect its magnitude (Fig. 6c). Increasing P/K controls the value of the hydraulic head and has a major effect on the associated SP (Fig. 6b).

Effect of the aquifer–basement interface

If the coupling coefficient C_s in the basement is different from C_2, to V_1 we must add the potential V_2 created by the basal interface of the lava flow

$$V_2 = \frac{(C_s - C_2)}{2\pi} \int_0^L \frac{[h(x') - h_s]H(x')}{(x - x')^2 + h^2(x')} \, dx', \tag{11}$$

and the potential V_3 created by the saturated part of the upstream limit

$$V_3 = \frac{(C_s - C_2)}{\pi}\left[\tan^{-1}\frac{h_s}{x} - \tan^{-1}\frac{L\sqrt{(P/K)}}{x}\right]. \tag{12}$$

Referring to the above discussion and choosing plausible values for C_s, ($C_2 \leq C_s < 1.5\ C_2$) affects the value of the SP anomaly (Fig. 6d) without notably changing its shape. Considering $C_s = C_2$ but slightly increasing C_2 would produce a similar SP. Without specific determination of C_2 and C_s, it appears useless to complicate the computation by assigning a contrast of coupling coefficients on this interface.

Effect of the contrast of conductivity

Let us consider a homogeneous lava flow drained by two zones of springs parallel to the $0y$-axis (Fig. 7). Between these two lines, the hydraulic head and the free surface are symmetrical with respect to the y–z plane and can be obtained from (8) and (9). We also neglect the slope of the water table, considering it as a horizontal plane located at depth $h(x)$. In each homogeneous zone the SP can be expressed as a Fourier integral:

$$\Psi_i(x, z) = \frac{2}{\pi}\int_0^{\infty} [A_i(\lambda)e^{\lambda z} + B_i(\lambda)e^{-\lambda z}] \cos \lambda x \, d\lambda, \tag{13}$$

where A_i and B_i are functions of λ and $i = 1, 2, 3$. We have the following boundary conditions: (1) On the ground surface the vertical density of current is zero. (2) on the water table the normal density of current is continuous. (3) On the aquifer–basement interface, the normal density of current is also continuous, but we assume that there is no contrast of coupling coefficient.

Using the boundary conditions and solving for the unknown functions A and B, we finally have the potential on the ground surface:

$$\Psi_{1(z=0)} = V = \frac{2}{\pi}\int_0^{\infty} 2A \cos \lambda x \, d\lambda, \tag{14}$$

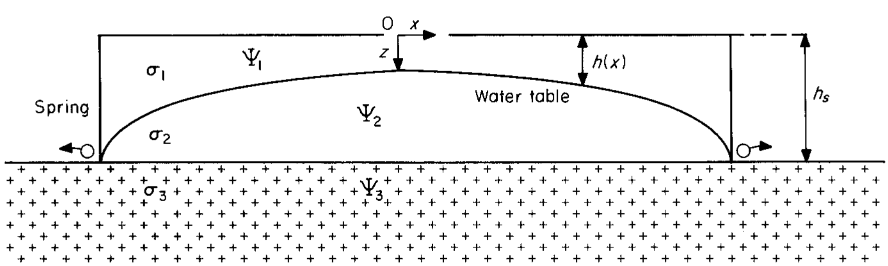

FIG. 7. Unconfined aquifer in a lava flow supplied by its own surface and drained by two parallel lines of springs; parameters presented according to the main text. The SP Fourier transform corresponding to each zone is indicated.

where

$$A = \frac{-g(\lambda)\sigma_2 R}{\sigma_1(e^{\lambda h(x)} - e^{-\lambda h(x)}) - \sigma_2(e^{\lambda h(x)} + e^{-\lambda h(x)})R}, \tag{15}$$

with

$$R = \frac{K + e^{-\lambda h(x)}}{K - e^{-\lambda h(x)}},$$

where

$$K = \frac{\sigma_3 - \sigma_2}{\sigma_3 + \sigma_2} e^{\lambda[-2h_s + h(x)]}.$$

$$g(\lambda) = \left(\frac{\pi}{2}\sqrt{\frac{P}{K}}\right)\left(LC\,\frac{J_1(L\lambda)}{L\lambda}\right) \tag{16}$$

is the Fourier transform of $h(x)$ and where the notations of Fig. 7 have been used.

Contrasting situations, such as $\rho_1 = 30\,000$ Ωm, $\rho_2 = 10\,000$ Ωm and $\rho_3 = 1000$ Ωm, create the same SP as if $\rho_1 = \rho_2 = \rho_3 = 10\,000$ Ωm or as obtained from (10). With large aquifers, compared to their vertical discontinuities, the resistivities in the different zones do not produce any effect on the SP values and do not need to be considered. It would be different for vertical flows and heterogeneties (volcanic dikes), as described by Fitterman (1979).

SP associated with the southern limit of the axial graben

High SP gradients have been observed on the southern limit of the axial graben (Figs 5 and 8) corresponding to the fault system delimiting it, as revealed by the resistivity soundings. These faults appear to be the upstream limit of the graben aquifer, as seen in the previous model. The water table in the graben is lower than the fault's upper block; the upper block is actively drained by the graben, and the hydraulic head is discontinuous between the two compartments. Resistivity soundings indicate desaturated pyroclastics of high resistivity in the upper block and a 50 m deep water table in the lower one. The hydraulic head baseline was chosen to correspond with the level of Argnat spring which drains the graben, e.g. $h_0 = 0$ and $h_s = 200$ m in (9) and (10). Equation (8) with $C_2 = 1.25$ mV/m and the appropriate geometrical parameters was integrated to compute a theoretical SP anomaly which fits remarkably well with the experimental one (Fig. 8c).

SP associated with palaeovalleys

Deep, narrow SP anomalies characterize the palaeovalleys' thalweg (Fig. 5). An SP profile across the Argnat palaeovalley shows two zones of high gradient with a parabolic anomaly in between, in superposition with a regular gradient due to the

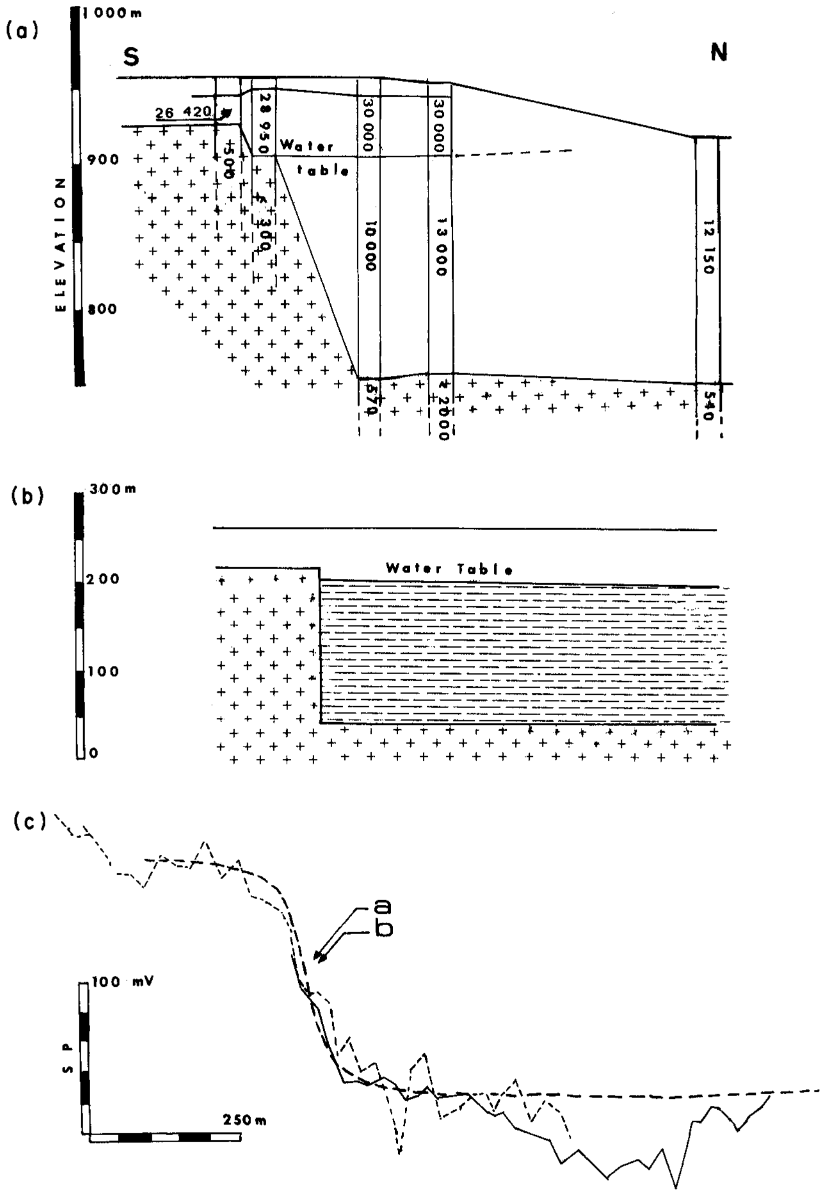

FIG. 8. (a) Cross-section of the southern limit of the axial graben according to resistivity sounding data. The vertical columns represent the resistivity sounding log, figures inside them indicate the true resistivity in Ωm, and the zone of crosses corresponds to the basement. (b) Proposed model for computations. The striped zone corresponds to the saturated zone of the volcanic aquifer, and the area of crosses represents the basement. (c) SP profiles 7 and 8 (also see Fig. 4) and theoretical curve obtained from the model in Fig. 8b with $C_2 = 1.25$ mV/m. The letters refer to the inflection points associated with the graben's limits and are plotted on Fig. 4.

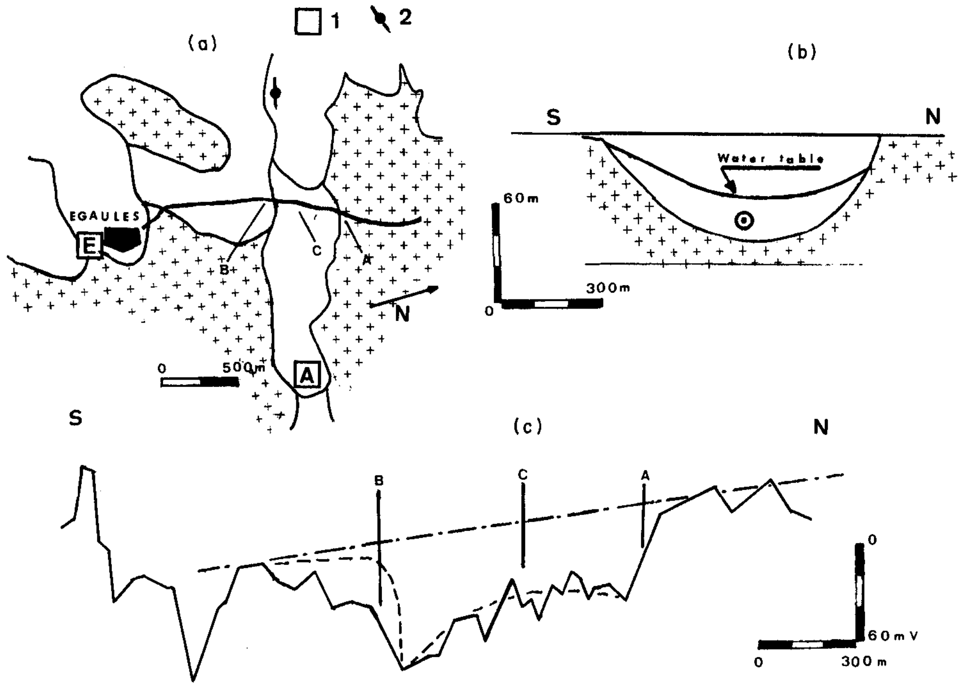

FIG. 9. (a) Location map of SP profile 3. The crosses indicate the basement. The symbols indicate: (1) spring or gallery [Argnat gallery; E: Egaules spring], (2) resistivity sounding S47. (b) Proposed model for the Argnat palaeovalley. (c) SP profile 3 (———) compared with the computed anomaly (– – –) obtained from the model presented in Fig. 9b. The letters indicate the position of the thalweg (C) and the flanks (A and B) of the palaeovalley. The same points are plotted in Fig. 9a.

neighbouring axial graben (Fig. 9). The northern high gradient zone corresponds to the north flank of the valley, as shown by the close basement outcrop. The opposite high gradient zone probably corresponds to the southern flank, masked by lava flows. Between these two zones, the SP curve represents the inverted shape of the water table, which is therefore assumed to be depressed along the thalweg. This could indicate a better transmissivity due to the thicker saturated zone in the thalweg. If we consider the surface of the lava flow, the thalweg line and the water table to be parallel to each other (all of them are gently sloping eastwards), we can use (8) to compute a theoretical SP anomaly. $H(x)$ is adjusted to produce a parabolic water table (Fig. 9b), with Argnat's spring level as baseline. For $C_2 = 1.25$ mV/m, the field values fitted perfectly.

SP helped to localize the Volvic thalweg below its volcanic cover (Fig. 5). Two profiles (Fig. 10) show the valley's anomaly superimposed on the graben's anomaly: the flank of the valley acts as a hydraulic sill, draining the graben's water without providing continuity of the hydraulic head from the graben to the valley. Thus, the graben and the valley act as two independent SP sources. The graben's contribution

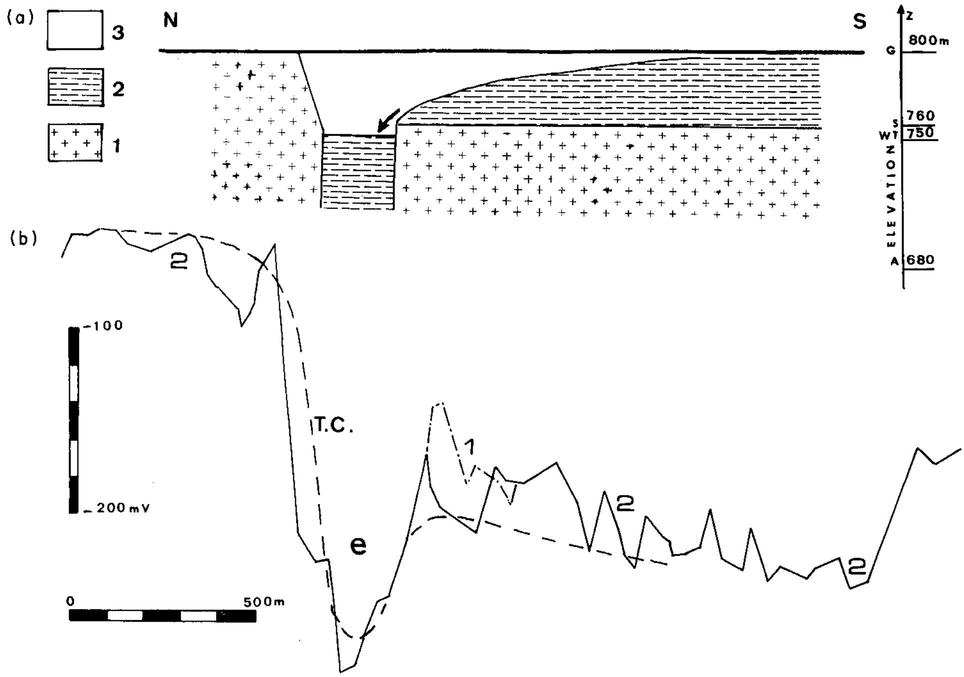

FIG. 10. SP anomaly associated with the Volvic palaeovalley and the axial graben. (a) Proposed model. The symbols indicate: (1) basement, (2) saturated zone of the volcanic aquifer, (3) desaturated zone. The elevation figures on the right refer to: A: Argnat gallery (reference level for the flow in the graben); WT: supposed water table in the palaeovalley; S: sill between the graben and the valley; G: ground level. (b) SP profiles 1 (—-—-) and (2) (———) (located on Fig. 4) compared with the computed anomaly (- - - -) obtained with the model presented in (a). The letter e designates the probable location on the thalweg and has been plotted on Fig. 4.

V_1 can be obtained from (8) with the appropriate parameters (Fig. 10a) and by taking Argnat's spring level as baseline for the hydraulic head [$h_0 = 80$ m and $h_s = 40$ m in (9) and (10). The SP produced by the valley can be obtained from

$$V_2 = \frac{-C_2}{2\pi} \int_0^L \frac{H(x')[(x-x')\,\mathrm{d}h/\mathrm{d}x' + h(x')]}{(x-x')^2 + h^2(x')} \left[\frac{y-y'}{\sqrt{(x-x')^2 + (y-y')^2 + h^2(x')}}\right]_{-e}^{e} \mathrm{d}x', \qquad (17)$$

derived from (7) with e representing half of the width of the valley. $H(x)$ and $h(x)$ can be obtained from (9) and (10) with $P/K = 10^{-2}$ (the valley is mainly supplied by the graben's water in addition to its own surface water). The Volvic spring level is the hydraulic head baseline for the valley's flow. For $C_2 = 1.25$ mV/m, adding V_1 and V_2 produces theoretical SP values close to the field SP.

Long SP profiles across the Chaîne des Puys

Three long profiles cross the Chaîne des Puys between Puy de Jûmes and Puy Chopine (Fig. 4):

Profile 4 (Fig. 11a) shows the lateral limits of the graben aquifer, associated with strong gradients (points a and h). Strongly negative values (down to −650 mV at b) and steep vertical gradients (up to 3 mV per metre of elevation) observed on the flank of Puy de Jûmes are probably due to the rising of the water table in the volcano, which is one of the upper points of the graben aquifer.

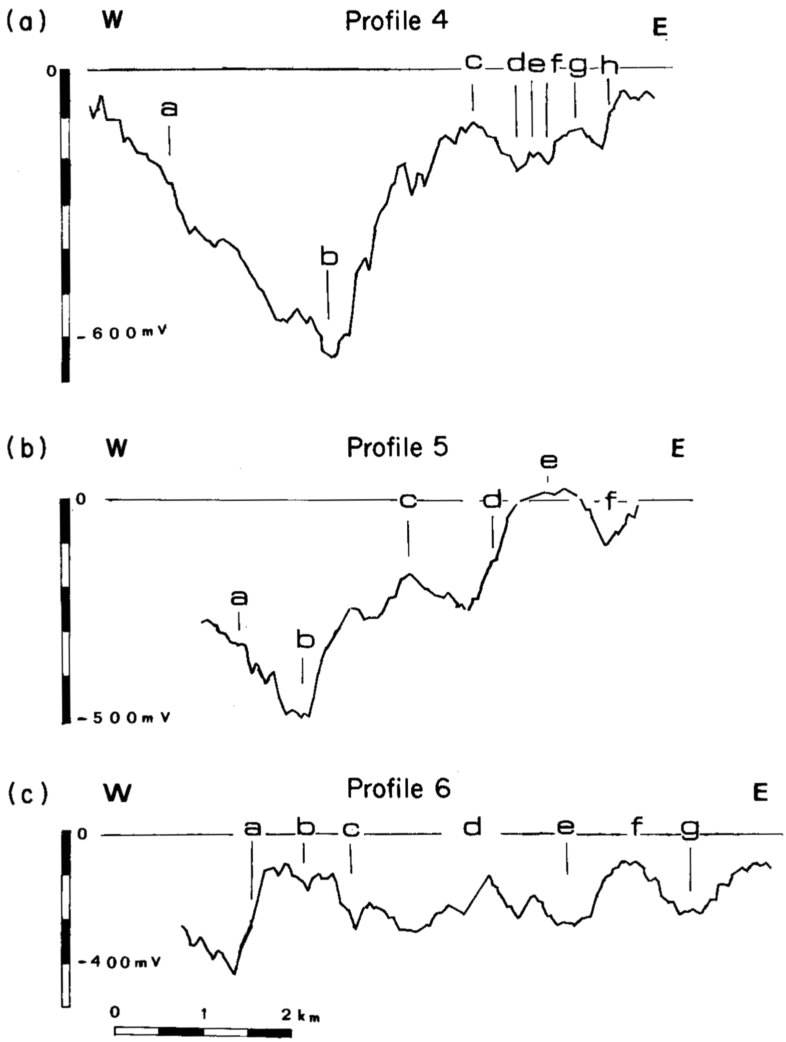

FIG. 11. Long SP profiles across the Chaîne des Puys. The figures and letters correspond to locations in Fig. 4 and to the description in the text.

Profile 5 (Fig. 11b) shows steep gradients associated with the limit of the aquifer (points a and d) and steeper ones on each flank of the volcanic range, down to a minimum on the pass in b. As in the Argnat palaeovalley and on Profile 4, the water table seems depressed along the axis of the graben, creating a relative maximum of SP around c. In the east, groundwater flow towards Egaules spring acts as an independent SP source with a minimum SP around point f. Values close to zero around e confirm the separation of the two basins, corresponding to a basement crest.

Profile 6 (Fig. 11c) indicates maximum SP (point b) on the trachytic plug of Chopine, which is probably an aquitard relief separating the basins of Fontêtes and Fontaine de Séranges from the graben aquifer. The western basins begin at point a and the graben aquifer is spread between c and d. Tributary, but separated, flows around point e generate their own SP anomaly. The upper part of the Egaules spring basin generates a third anomaly (point g) separated from the previous one by an SP maximum around point f, probably corresponding to a basement crest.

To compare the field values with theoretical anomalies, we had to develop a conformal transformation to account for the volcanic topography. Let us suppose that the volcanic range and the underground flow pattern are invariant along the 0y-axis, and consider two complex numbers $Z = x + \mathrm{i}z$ and $\zeta = \mu + \mathrm{i}\eta$. ζ is related to Z through the following conformal transformation:

$$Z = \zeta + \frac{h}{\zeta - \mathrm{i}a}, \tag{18}$$

thus

$$x = \mu\left(1 + \frac{h}{\mu^2 + (\mu - a)^2}\right)$$

and

$$z = \eta - \frac{h(\eta - a)}{\mu^2 + \eta - a)^2} \tag{19}$$

For $\eta = 0$ (ground surface in the transformed coordinates system), h and a control the height and width of a bell-shaped curve which can roughly represent a volcanic range (Fig. 12b). The conformal transformation (20) reciprocal to (18) lets us compute the coordinates of the water table in the (μ, η) system.

$$\zeta^2 - \zeta(\mathrm{i}a + z) + h + \mathrm{i}az = 0, \tag{20}$$

thus

$$\left.\begin{aligned} \mu &= \frac{x \pm \sqrt{\rho}\cos\theta/2}{2} \\ &\text{and} \\ \eta &= \frac{(z - a) \pm \sqrt{\rho}\sin\theta/2}{2}, \end{aligned}\right\} \tag{21}$$

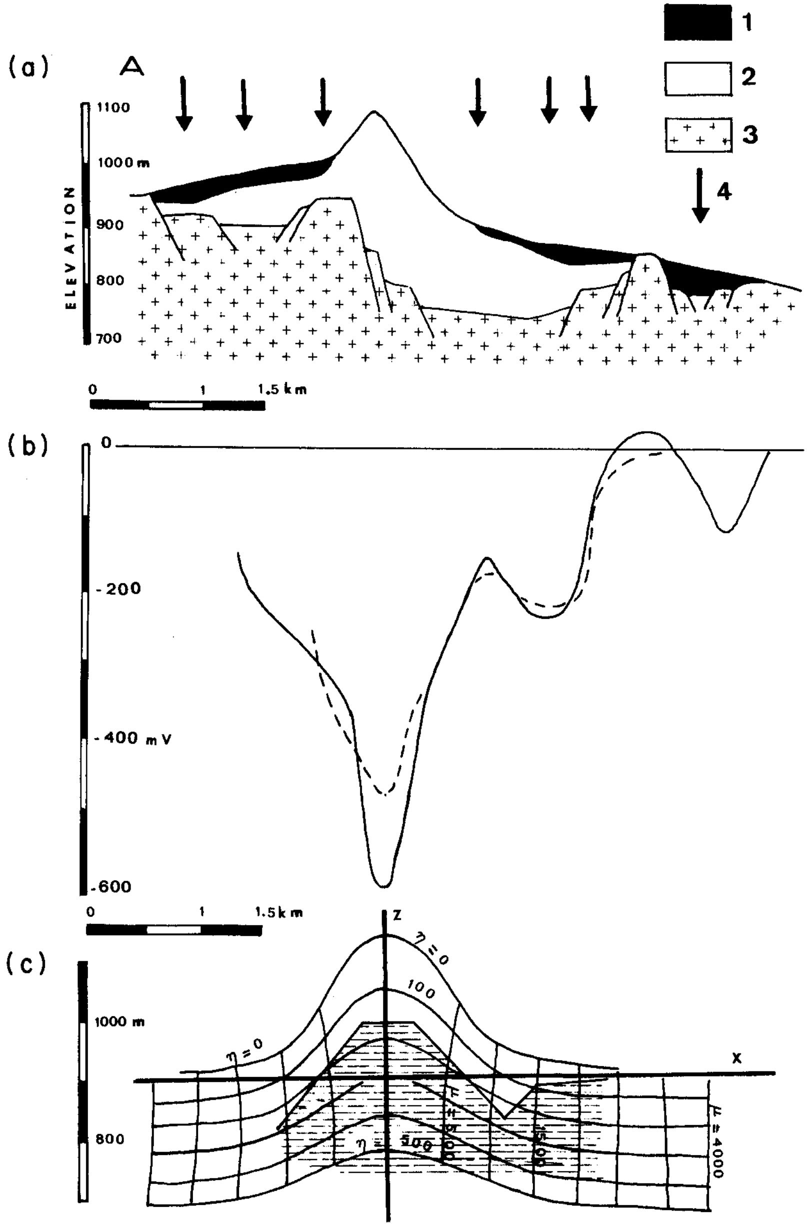

FIG. 12. (a) Cross-section profile of the northern part of the Chaîne des Puys (see the A–B line on Fig. 4) according to the resistivity sounding data. The symbols indicate: (1) basalt laval flow outcrops, (2) undifferentiated volcanic formations, (3) basement, (4) location of the resistivity soundings. (b) Comparison between the SP profile along A–B (solid line) and the computed values (dashed line) obtained with the model presented in Fig. 12c. (c) Representation of the conformal transformation used for the computation. The striped area corresponds to the saturated zone proposed as the model for computation.

where

$$\rho = x^2 - 4h + (z - a)^2$$

and

$$\theta = \tan^{-1} \frac{2x(z - a)}{x - (z - a) - 4h}.$$

We keep only the root belonging to the half-space representing the ground. Using (10) in the (μ, η) system and choosing $C_2 = 1.9$ mV/m, field values can easily be represented by a model characterized by an important rise in the water table, in the volcanic range, which acts as an underground watershed, and by a drainage axis (depression of the water table) in the central part of the graben (Fig. 12c).

Interpretation of the SP map

The different cases observed and described above are gathered together in Table 2, which is a guideline for the interpretation of the SP map presented in Fig. 5. We can see that SP entirely confirms the results obtained from resistivity soundings (interdependency of the Argnat–Volvic system, independence of other systems), but considerably improves the accuracy of delimitation of these different systems. Other information is specifically produced by the SP method, such as the location of drainage axes, palaeovalleys, and the underground watershed role of certain Strombolian volcanoes. Boundary and drainage conditions are therefore revealed by SP.

Hydrogeological Synthesis

Geophysical methods succeed in delimiting the different hydrogeological basins under the volcanic cover. In places where the basement outcrops, the water flow is limited to runoff or shallow flows, both of which are controlled by the surface topography in the survey area. Basement runoff flowing along a lava flow usually infiltrates into it and supplies some of the springs of the volcanic aquifers. Runoff is null on the volcanic covers. Table 3 summarizes the basins' characteristics. We can see that the ratio of the discharge of Volvic and Argnat (2.35) is close to the surface of their respective basins (2.25), which is easily understood as they are subject to similar climatic conditions. Otherwise, estimating the annual rainfall from the closest rain gauges, with a plausible evapo-transpiration rate (42%), we obtain an equivalent hydrological balance for the basins whose discharge is known.

Barbaud (1983) showed that groundwater flowing through lava flows had a smaller content of minerals and, therefore, a lower conductivity than water flowing through pyroclastics. Table 3 shows that the conductivity of the spring water reflects the proportion of lava flow in its basin. His ^{18}O isotope analyses indicate a mean altitude of infiltration of 1040 m for Argnat and 800 m for Volvic, which agree with our delimitations.

TABLE 3. Hydrogeological characteristics and water balance of the studied basins.

System	Argnat	Egaules	Louchadière	Volvic	Total
Surface in pyroclastics	7.9 (44%)	0	1 (20%)	7.8 (11%)	16.7 km^2
Surface in basaltic lava flow	6.75 (38%)	1.3 73%	3.2 (65%)	20 (68%)	31.2 km^2
Surface in trachytes	0.85 (5%)	0	0	0	0.85 km^2
Surface in basement	2.31 (13%)	0.5 27%	0.7 (14%)	12.3 (21%)	15.8 km^2
Total surface	17.8 km^2	1.8 km^2	4.9 km^2	40 km^2	64.5 km^2
Mean yield (m^3/s)	0.230	Unknown	0.080	0.540	0.850
Estimated rainfall (mm/year)	970	970	1 226	970	—
Computed yield	0.230	—	0.080	0.520	—
Water conductivity	144 μS/cm	91 μS/cm	102 μS/cm	115 μS/cm	—

CONCLUSIONS

Systematic SP exploration of large areas has provided significant and specific hydrogeological information. SP is a particularly powerful method as it is the only one depending directly on the groundwater flow itself. With unconfined aquifers, the water table appears to be the main source of SP anomalies, and these reproduce its inverted shape.

Poorly mineralized waters creating relatively large values of the coupling coefficient *C*, and important well-delimited aquifers are both responsible for large, characteristic, SP anomalies on the Chaîne des Puys. Testing the method on other aquifers and accurately determining the coupling coefficient for different zones would help to develop the method and define its limitations.

Elsewhere, the information provided by the SP method is consistent with resistivity and hydrogeochemistry surveys. But SP provides more accurate information. The association of these methods succeeded in answering the major preoccupation of the sponsor by revealing the boundary of the catchment area for each spring, indicating the axial graben as the major groundwater reservoir, and delineating possible zones of greater vulnerability to pollution, such as the palaeovalley's thalweg.

ACKNOWLEDGEMENTS

The author thanks M. Aubert, Physicien Adjoint at the Observatoire de Physique du Globe de Clermont-Ferrand, his thesis director, for his considerable assistance and G. Vasseur, Research Director at Centre National de la Recherche Scientifique, for his help in the mathematical approach to the SP model; A. Rongères, Director of the Hydrology Service; and J. Chanut and J. C. Dupuy, of the Direction Departementale de l'Agriculture du Puy-de-Dôme, for having supplied considerable advice and data. The surveys were sponsored by the Ministère de l'Agriculture. This publication must be considered a common contribution from the two institutions with which the author was affiliated: the Observatoire de Physique du Globe de Clermont-Ferrand and the Centre Géologique et Géophysique, Université des Sciences et Techniques du Languedoc, Montpellier.

References

AHMAD, M.U. 1961. A laboratory study of streaming potentials. *Geophysical Prospecting* **12**, 49–64.

AUBERT, M. and CAMUS, G. 1974. Structures profonde de la Chaîne des Puys. *Bulletin Volcanologique* **38**, 445–457.

AUBERT, M., CAMUS, G. and FOURNIER, C. 1984. Resistivity and magnetic surveys in groundwater prospecting in volcanic areas – case history Maar of Beaunit, Puy de Dôme, France. *Geophysical Prospecting* **32**, 554–563.

BARBAUD, J.Y. 1983. Etude chimique et isotopique des aquifères du Nord de la Chaîne des Puys. Thèse de troisième cycle, Université d'Avignon.

BELEKESSA, R. 1977. Hydrogéologie de la Chaîne des Puys. Thèse de Diplome d'Etude Superieures Specialisées, Université de Clermont-Ferrand.

CAMUS, G. 1975. La Chaîne des Puys (Massif Central Français). Etude structurale et volcanologique. Thèse de doctoroat d'état, Université de Clermont-Ferrand.

COROMP, P., ROBACH, M., LAUNAY, M. and GIGNOUX, M. 1974. Possibilitiés d'étudier des écoulements souterrrains à partir des champs magnétiques et des distributions de potentials spontanés provoqués à la surface du sol par des courants d'électro-filtration. Raport CEA/CENG, Grenoble, published by the Comissariat à L'Energie Atomique, Centre d'Etudes Nucléaires de Grenoble, Grenoble, France.

FITTERMAN, D.V. 1978. Electrokinetic and magnetic anomalies associated with dilatent regions in a layered earth. *Journal of Geophysical Research* **83**, 5924–5934.

FITTERMAN, D.V. 1979. Calculations of self potentials anomalies near vertical contacts. *Geophysics* **44**, 195–205.

FOURNIER, C. 1983. Methodes géoelectriques appliquées à l'hydrogéologie en région volcanique (Chaîne des Puys, Massif Central Français), développments de la méthode des potentials spontanés en hydrogéologie. Thèse de troisième cycle, Université de Montpellier II.

GUILLAUME, A. 1977. Analyse des variables régionalisées, *Traitement du signal en sciences de la Terre.* Doin Publishers, Paris.

OGILVY, A.A., AYED, M.A. and BOGOLOVSKY, V.A. 1969. Geophysical studies of water leakage from reservoirs. *Geophysical Prospecting* **28**, 792–804.

SCHOELLER, H. 1962. *Les Eaux Souterraines.* Masson Publishers, Paris.